Properties of self-interstitials in cubic metals: Static displacements

P. N. Ram
Department of Physics, North-Eastern Hill University, Shillong 793 003, Meghalaya, India
(Received 2 February 1990; revised manuscript received 19 July 1990)

We study the problem of self-interstitials in face-centered- and body-centered-cubic crystals using defect models that include force-constant changes extending up to second neighbors of the defect site. Complete group-theoretic analysis of defect models for the ⟨100⟩ dumbbell in a fcc lattice and the ⟨110⟩ dumbbell in a bcc lattice are presented. We apply the results to the calculation of the static-displacement field of ⟨100⟩-split interstitials in the fcc metals Cu, Ag, Au, Ni, and Al and ⟨110⟩-split interstitials in the bcc metals Fe, Mo, and W with the use of the Green's-function method of lattice statics. The calculated results for the displacement field, relaxation volume, dipole tensor, and formation energy are compared with those from computer-simulation studies and lattice-statics calculations.

I. INTRODUCTION

The properties of self-interstitial atoms (SIA's) in metals are of considerable interest for an understanding of the problem of radiation damage in metals. One of the most important properties of the self-interstitials is elastic interaction between them and naturally much effort has been made to understand the structure, energies, and induced strain field of these point defects. Over the years, owing to concerted effort, both theoretical and experimental, many controversial questions—notably the structure and energies—have been settled and new insight concerning the dynamical behavior of these point defects has been gained. However, the study of dynamical properties of SIA's is confined to fcc metals only. The split or dumbbell interstitial seems to be the most stable configuration in cubic metals as evidenced by computer-simulation studies in fcc metals[1–4] and bcc metals.[5–9] The axis of the dumbbell lies along the ⟨100⟩ direction in fcc metals, whereas it is along ⟨110⟩ in bcc metals. The dumbbell configuration is confirmed by measurements using different experimental techniques in both fcc and bcc metals.[10] In any case, the dumbbell model of self-interstitials can be understood even in cases of notable exceptions like Au and superconducting bcc metals Nb, V, and Ta.[11]

In most of the theoretical studies concerning the properties of the SIA's computer simulation using empirical pair potentials has been employed. Following the detailed computer experiment of Scholz and Lehmann[3] on copper the dynamics of self-interstitials in fcc metals has been discussed at length, with special emphasis on the resonant modes of self-interstitials which are instrumental in explaining physical properties of irradiated metals.[12–15] Contrary to static properties, the dynamical properties of the defects are usually discussed within the framework of the Green's-function theory, utilizing a localized perturbation model where the interaction of the defect is supposed to extend to a few neighbors of the defect. The localized defect model can also be used for static properties of defects, employing the method of lattice statics, especially the Green's-function method[16] which runs parallel to the method of defect-lattice dynamics. In a defect-lattice statics or dynamics calculation the basic quantity involved is the lattice Green's function for the defect lattice. Even with the localized perturbation model the work is quite laborious as there are a large number of degrees of freedom necessitating inversion of large matrices and as such group-theoretic techniques are used to exploit the point symmetry of the defect site, resulting in block diagonalization of matrices. A typical calculation involves the following: construction of an ideal lattice Green's-function matrix, a perturbation matrix, the determination of symmetry coordinates pertaining to the point group of the defect site, and block diagonalization of these matrices apart from the actual numerical computation of different quantities.

The Green's-function theory for substitutional impurities has been developed to a considerable extent and has become a powerful and practical tool for solving the crystal-impurity problem in the low-concentration approximation to a high degree of precision.[17–19] Applications of the method to various impurity-host systems have generated a great deal of information, and as a result, considerable insight into the vibrational properties of substitutional impurities has been gained. Because of the complexity of the self-interstitial problem from a computational point of view, only rather idealized situations have been considered. For instance, in almost all lattice-dynamical calculations performed so far,[20–26] a simplified nearest-neighbor defect model for the ⟨100⟩ dumbbell has been employed and in many cases group theory was not used.[23,24] Though the use of group theory is not absolutely necessary and with availability of high-speed computers much larger matrices can be handled easily, a group-theoretic analysis is still useful and desirable as it not only reduces the computational problem, it also helps to understand the physics involved in the problem. As far as the resonant vibrations of the SIA's are concerned a nearest-neighbor model seems to be ade-

quate, but it is quite inadequate in describing the vibrations of the neighbors of the dumbbell atom such that it fails to give the so-called B-mode resonances which involve the vibrations of the neighbors only.[21,27] Evidently any detailed comparison of any calculated physical property with experimental results calls for the consideration of a more extended defect model for such strongly perturbing defects like dumbbell interstitials.

In view of the above, in order to undertake a systematic study of properties of self-interstitials in cubic metals, the present paper is mainly devoted to the analysis of second-neighbor defect models for the ⟨100⟩ dumbbell in fcc metals and the ⟨110⟩ dumbbell in bcc metals, where results of detailed group-theoretical analysis are presented. While reporting the present results we believe that they would be of much use in future applications and note that, except for the group-theoretic analysis for the ⟨100⟩ dumbbell in the fcc lattice by Ludwing[28] who has considered a defect model consisting of first neighbors and two second-neighbor atoms lying along the dumbbell axis, no such analysis has been reported. In fact, the studies on the dynamics of self-interstitials in bcc metals are still lacking.

As a first application of these models we calculate the static displacement fields and related properties of these self-interstitials in a number of fcc and bcc metals. Bullough and Tewary[29] used the Green's-function method to calculate distortion around the ⟨100⟩ dumbbell in Cu using the Born-Mayer potential. The calculation gave the equilibrium position of the dumbbell atom in agreement with earlier computer-simulation results while the displacement of neighbors was found to be considerably different. On the other hand, if we compare the displacement field in Cu reported by Miller and Heald[30] employing the Kanzaki method[31] with the computer-simulation result of Schober,[32] both using the Morse potential, we find that these results are more or less similar. However, there is a serious discrepancy in that the displacement of the nearest axial atom to the dumbbell is opposite in sign to that found in computer-simulation results. Evidently, it is of some interest to consider the lattice-statics calculation of distortion around self-interstitials in fcc metals. As far as bcc metals are concerned there is no lattice-statics calculation of static properties of self-interstitials. The present calculation, therefore, aims at a comparative study of lattice statics and computer-simulation results. We have used the truncated Morse potential for the fcc metals Al, Cu, Ag, Au, and Ni and potentials constructed by Johnson and Wilson[33] (JW) for the bcc metals Fe, Mo, and W.

II. GENERAL THEORY

The standard Green's-function theory for the isolated point defects is well developed.[17] In the case of interstitials additional degrees of freedom are introduced in the lattice and an alternative formulation of the defect problem proposed by Krumhansl and Matthews[34] is found to be more suitable. In this approach the vibrational problem of the lattice with defects is viewed as an eigenvalue problem similar to the perfect lattice but with changed values of some of the elements of the dynamical matrix. The method has been fully discussed by Dederichs and Zeller[22,35,36] and Ram and Dederichs.[23,24] The Green's function of the defect lattice containing only one interstitial atom is

$$(\Phi - M\omega^2)G(\omega) = 1 \ , \tag{1}$$

while that of the ideal lattice is given by

$$(\mathring{\Phi} - \mathring{M}\omega^2)\mathring{G}(\omega) = 1 \ , \tag{2}$$

where Φ ($\mathring{\Phi}$) and M ($\mathring{M}$) are the force-constant and mass matrices for the defect (ideal) lattice. We divide the whole space of all atoms into a central subspace C containing the interstitial and a subspace R containing the remaining atoms. We partition the matrices Φ, M, and G so that Eq. (1) becomes

$$\begin{bmatrix} \Phi_{CC} - M_{CC}\omega^2 & \Phi_{CR} \\ \Phi_{RC} & \Phi_{RR} - M_{RR}\omega^2 \end{bmatrix} \begin{bmatrix} G_{CC} & G_{CR} \\ G_{RC} & G_{RR} \end{bmatrix} = \begin{bmatrix} 1 & 0 \\ 0 & 1 \end{bmatrix} . \tag{3}$$

The Green's functions G_{CC}, G_{CR}, G_{RC}, and G_{RR} can easily be determined. The result is

$$\begin{aligned} G_{CC} &= (\Phi_{CC} - \Phi_{CR}\hat{G}_{RR}\Phi_{RC} - M_{CC}\omega^2)^{-1} \ , \\ G_{RR} &= (\Phi_{RR} - \Phi_{RC}\hat{G}_{CC}\Phi_{CR} - M_{RR}\omega^2)^{-1} \ , \\ G_{CR} &= -G_{CC}\Phi_{CR}\hat{G}_{RR} \ , \\ G_{RC} &= -\hat{G}_{RR}\Phi_{RC}G_{CC} = G'_{CR} \ , \end{aligned} \tag{4}$$

where G'_{CR} is the transposition of G_{CR}. The Green's function $\hat{G}_{RR} = (\Phi_{RR} - M_{RR}\omega^2)^{-1}$ describes vibrations of the lattice when the interstitial is held fixed, whereas the $\hat{G}_{CC} = (\Phi_{CC} - M_{CC}\omega^2)^{-1}$ describes the Einstein vibration of the interstitial. The defect Green's function $G_{CC}(\omega)$ determines the local density of states of the interstitial atom. Evidently the term $\Phi_{CC} - \Phi_{CR}\hat{G}_{RR}\Phi_{RC}$ gives the effective coupling of the defect when it is embedded in the lattice, the correction $-\Phi_{CR}\hat{G}_{RR}\Phi_{RC}$ to the Einstein force constant Φ_{CC} represents the effect of the dynamic relaxations of the atoms in the host lattice. The function $\hat{G}_{RR}$, which enters the expressions for G_{CC}, G_{CR}, and G_{RC}, can easily be evaluated in terms of the ideal lattice Green's function $\mathring{G}$:

$$\hat{G}_{RR} = \mathring{G} - \mathring{G}V_{RR}\hat{G}_{RR} = \mathring{G} - \mathring{G}\hat{t}\mathring{G} \ , \tag{5}$$

where

$$\begin{aligned} \hat{t} &= V_{RR}(1 + \mathring{G}V_{RR})^{-1} \ , \\ V_{RR} &= \Phi_{RR} - \mathring{\Phi} - (M_{RR} - \mathring{M})\omega^2 \ . \end{aligned} \tag{6}$$

The Green's function G_{RR} is especially useful for the macroscopic properties of the defect lattice since it gives the vibrations of the host lattice in the presence of the interstitial by eliminating the additional degrees of freedom introduced by it. The elimination of the interstitial coordinates leads to an effective coupling between the lattice atoms. The term $-\Phi_{RC}\hat{G}_{CC}\Phi_{CR}$ represents the intersti-

tial reaction to the host system. Again G_{RR} can be calculated by the standard Green's-function method

$$G_{RR}=(\mathring{\Phi}+\tilde{V}_{RR}-M\omega^2)^{-1}=\mathring{G}-\mathring{G}\tilde{V}_{RR}G_{RR}\ , \tag{7}$$

if we add to the perturbation the interstitial induced interaction between the host atoms

$$\tilde{V}_{RR}=V_{RR}-\Phi_{RC}\hat{G}_{CC}\Phi_{CR}\ . \tag{8}$$

Very often only the Green's functions G_{CC} and/or G_{RR} are needed. The major part of the calculation is to determine the matrix $1+\mathring{G}V_{RR}$ and $1+\mathring{G}\tilde{V}_{RR}$ and invert them. Using group-theoretic arguments these matrices are calculated for different irreducible subspaces of the defect space.

III. CALCULATION FOR ⟨100⟩ DUMBBELL IN A fcc LATTICE

The ⟨100⟩-dumbbell configuration in a fcc lattice is shown in Fig. 1. As is clear from the figure, the center of the dumbbell is at a normal lattice site formerly occupied by one of the dumbbell atoms. We assume a vacancy at the center of the dumbbell, which is taken to be origin, and as such the defect is described by an "assumed vacancy" and two interstitial atoms at $(0,0,\pm d)$, where $2d$ is the distance between the dumbbell atoms. The dumbbell is surrounded by 12 nearest neighbors and 6 second neighbors, which makes the defect space of 21 sites and one has to deal with 63×63 matrices.

The interaction between two atoms at a distance R is given by two usual force constants derived from the central potential $\Phi(r)$, a central-force constant $A=d^2\Phi/dR^2$, and a noncentral-force constant $B=(1/R)(d\Phi/dR)$. We consider seven types of force constants A_i,B_i $(i=1,2,\ldots,7)$ characterized by interactions between dumbbell atom 1 and atoms $\bar{1}$, 4, $\bar{4}$, 2, 10, 8, and $\bar{10}$ (see Fig. 1). The vacancy is described by zero

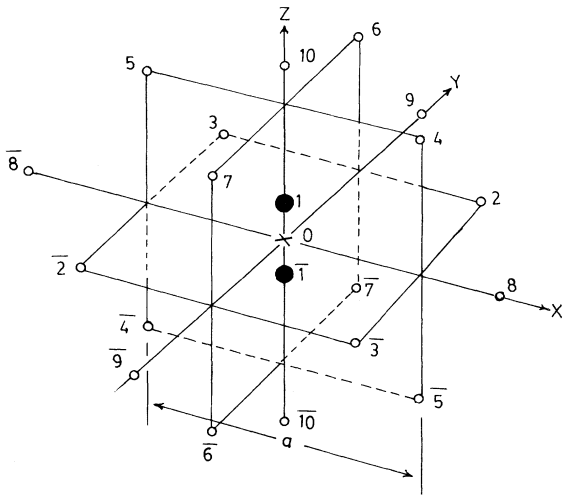

FIG. 1. Defect space for a ⟨001⟩ dumbbell in a fcc lattice.

coupling to its neighbors. All other force constants are assumed to be the same as in the ideal lattice and longer-ranged force-constant changes are neglected. In the presence of a strongly perturbing defect such as split interstitials, the host atoms in the defect space experience considerable lattice relaxation and hence the interactions between different atoms within defect space and that between these atoms and their neighbors are altered; all such changes in force constants are ignored in the present treatment. The force constants in the ideal lattice are given by A_1^0,B_1^0 and A_2^0,B_2^0 referring to first- and second-neighbor distances, respectively. In order to calculate the different force constants use is made of the formula[17]

$$\Phi_{\alpha\beta}(l,l')=\left[\frac{x_\alpha x_\beta}{r^2}\left[\Phi''(r)-\frac{1}{r}\Phi'(r)\right]+\frac{\delta_{\alpha\beta}}{r}\Phi'(r)\right]\Bigg|_{r=x(l,l')}\ , \tag{9}$$

$$\Phi_{\alpha\beta}(l,l)=-\sum_{l'}\Phi_{\alpha\beta}(l,l')\quad(l\neq l')\ , \tag{10}$$

so that the force-constant matrices can be expressed in terms of the usual central- and noncentral-force constants A_i,B_i.

Having determined the force constant matrices Φ and $\mathring{\Phi}$, the perturbation matrices V_{RR} or $\tilde{V}_{RR}$ are obtained in a straightforward way [Eqs. (6) and (8)]. The elements of the Green's-function matrix $\mathring{G}$ follow the symmetry of the ideal lattice which restricts the number of distinct nonzero elements. The elements of $\mathring{G}$ needed in the present defect model are 19 in number.

Apart from destroying the translational symmetry of the lattice complex, defects like split interstitials cause a reduction in the site symmetry from the cubic (O_h) to some group of lower order. For the present case of the ⟨100⟩ dumbbell the point-group symmetry is tetragonal (D_{4h}). The Cartesian components of the amplitudes of the displacements of the atoms from their equilibrium positions in the defect space provide basis functions for the reducible representation of the point group D_{4h}. We form a 63-dimensional column vector $U(n)$ taking these amplitudes as elements. The components of vector $U(n)$ can be expressed in terms of Cartesian or symmetry coordinates. The symmetry coordinates provide basis functions for irreducible representations of the point group and have been obtained[37] by the standard projection technique.[38] The total representation is decomposed into irreducible representations

$$\Gamma(D_{4h})=6A_{1g}+3A_{2g}+4B_{1g}+3B_{2g}+7E_g+A_{1u}+7A_{2u}+2B_{1u}+3B_{2u}+10E_u\ . \tag{11}$$

In addition to simplifying the calculations the symmetry coordinates are useful in identifying the characteristic defect modes (resonant and localized) according to different irreducible representations.

The symmetry coordinates are used to block diagonalize the defect matrices Φ, V_{RR}, and the Green's-function matrix $\mathring{G}$ according to different irreducible representa-

tions; the results are too lengthy to be reproduced here. However, from the symmetry coordinates it is readily observed that the displacements of the dumbbell atoms involve only four different irreducible representations: A_{1g}, E_g, A_{2u}, and E_u. This fact can, for example, be utilized in discussing the local density of states of the defect.

IV. CALCULATION FOR ⟨100⟩ DUMBBELL IN A bcc LATTICE

The ⟨100⟩-dumbbell configuration in a bcc lattice is shown in Fig. 2. As shown in the figure the center of the dumbbell is at the normal lattice site formerly occupied by one of the dumbbell atoms. Like the fcc case we consider a second-neighbor model where we assume a vacancy at the center of the dumbbell, which is taken as the origin of the coordinate system so that the defect is an assumed vacancy flanked by two interstitial atoms at $(\pm d, \pm d, 0)$. In a bcc lattice the second-neighbor distance is slightly larger than the first-neighbor distance and, therefore, this may be thought to be the simplest defect model. The dumbbell is surrounded by eight nearest neighbors and six second neighbors and as such the defect space consists of 17 sites and one has to deal with 51×51 matrices.

We consider seven types of force constants A_i, B_i $(i=1,2,\ldots,7)$ characterized by interactions between dumbbell atom 1 and atoms $\bar{1}$, 2, 4, $\bar{2}$, 6, $\bar{6}$, 8 (see Fig. 2). The force-constant matrices are determined in terms of these central- and noncentral-force constants, A_i, B_i. Apart from these force constants we need ideal lattice force constants A_1^0, B_1^0 and A_2^0, B_2^0 which refer to first- and second-neighbor distances, respectively. Similar to the ⟨100⟩ dumbbell in a fcc lattice, the assumed vacancy is described by zero coupling to the neighbors and possible force-constant changes between host atoms in the defect space and all other distant force constants are ignored. With the help of the force constants outlined above the force-constant matrices Φ, $\mathring{\Phi}$, and then the perturbation matrices are obtained. The elements of the Green's-function matrix needed in the present defect model are 16 in number.

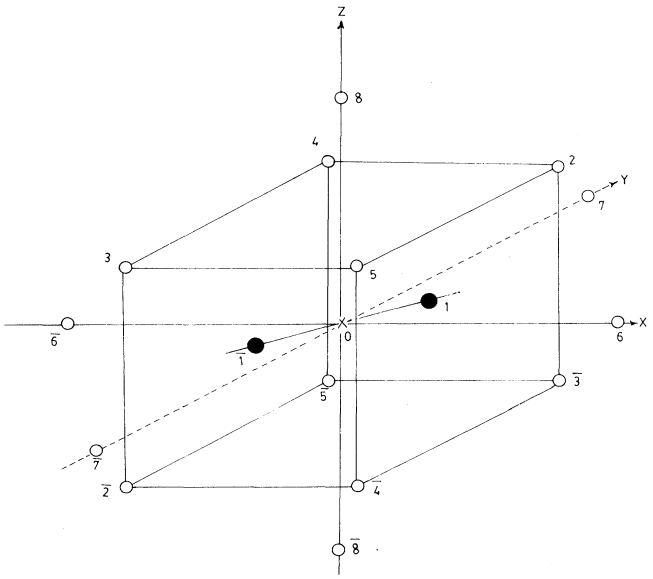

FIG. 2. Defect space for a ⟨110⟩ dumbbell in a bcc lattice.

In the present case of ⟨110⟩-split interstitials the site symmetry is reduced from cubic to orthorhombic (D_{2h}). The total defect space is decomposed into its different irreducible subspaces according to irreducible representations of the point group D_{2h},

$$\Gamma(D_{2h})=8A_g+5B_{1g}+6B_{2g}+5B_{3g}+3A_u +8B_{1u}+8D_{2u}+8B_{3u}\ . \tag{12}$$

The required symmetry coordinates have been obtained.[37] Using symmetry coordinates the Green's-function matrix and perturbation matrices are block diagonalized and detailed results for different irreducible representations have been obtained. However, the results are too lengthy to be reproduced here. From the symmetry coordinates it is observed that the motion of the dumbbell atoms figure in six irreducible representations: A_g, B_{1g}, B_{2g}, B_{1u}, B_{2u}, and B_{3u}. Such identification is quite helpful in discussing the vibrations of the dumbbell through the local density of states which clearly projects possible resonance and localized modes involving dumbbell atoms.

V. STATIC DISPLACEMENTS

In order to calculate the static displacements of atoms around the SIA's we use the Green's-function method of lattice statics as formulated by Tewary.[16] We consider the lattice with defects at absolute zero. With the presence of defects the crystal energy is changed in two ways: the defect interacts directly with the host atoms through a pairwise potential $\hat{\Phi}(r)$ and the host atoms are displaced from their equilibrium positions. If the atomic displacements are assumed to be small then the potential energy of the crystal can be expanded as a Taylor series,

$$\Phi=\sum_l \hat{\Phi}(l)+\Phi_0+\sum_{\alpha,l}\Phi_\alpha(l)d_\alpha(l) +\tfrac{1}{2}\sum_{\substack{l,l'\\ \alpha,\beta}}\Phi_{\alpha\beta}(l,l')d_\alpha(l)d_\beta(l')+\cdots\ , \tag{13}$$

where $\Phi_\alpha(l)$ is the derivative of Φ with respect to displacement $d_\alpha(l)$ evaluated at an equilibrium position of atoms. Minimizing the potential energy with respect to displacements, we have

$$0=\Phi_\alpha(l)+\sum_{l',\beta}\Phi_{\alpha\beta}(l,l')d_\beta(l') =-F_\alpha(l)+\sum_{l',\beta}\Phi_{\alpha\beta}(l,l')d_\beta(l')\ , \tag{14}$$

where $F_\alpha(l)$ is the force exerted by the defect on atom l. We can solve Eq. (14) for static displacements to get

$$d_\alpha(l)=\sum_{l',\beta}(\Phi^{-1})_{\alpha\beta}(l,l')F_\beta(l') \ . \tag{15}$$

It is noted that Φ^{-1} is the static lattice Green's function $G(\omega=0)$ [Eq. (1)] of the defect lattice and we write

$$d_\alpha(l)=\sum_{l',\beta}G_{\alpha\beta}(l,l')F_\beta(l') \ . \tag{16}$$

Using Eq. (14) in Eq. (13) we find the formation energy to be

$$E_f=\Phi-\mathring{\Phi}=\sum_l\hat{\Phi}(l)-\tfrac{1}{2}\sum_{l,\alpha}F_\alpha(l)d_\alpha(l) \ , \tag{17}$$

where the second term is the relaxation energy.

Another quantity of interest is the dipole tensor defined by[39]

$$P_{\alpha\beta}=\sum_l F^*_\alpha(l)R_\beta(l) \ , \tag{18}$$

where $F^*_\alpha(l)$ is the so-called Kanzaki force, i.e., the force at the site l at its relaxed position. The relaxation volume is calculated in terms of the dipole tensor

$$\Delta V=\mathrm{Tr}P/3K \ , \tag{19}$$

where K is the bulk modulus.

A. ⟨100⟩ dumbbell in a fcc lattice

The force $F_\alpha(l)$ on atom l is calculated by

$$F_\alpha(l)=-\sum_{l'}\Phi_\alpha(l,l')$$

$$=-\sum_{l'}\frac{x_\alpha}{r}\Phi'(r)\bigg|_{r=x(l,l')} \quad (l\neq l') \ . \tag{20}$$

The forces on different atoms in the defect space can be represented in terms of the following independent elements: $f_1=F_z(0,0,x)$, $f_2=F_y(0,1,1)$, $f_3=F_z(0,1,1)$, $f_4=F_x(1,1,0)$, $f_5=F_z(0,0,2)$, and $f_6=F_y(0,2,0)$.

We use the symmetry coordinates to project the forces in different irreducible subspaces of the defect space. The nonzero value comes only in the case of A_{1g} irreducible representation with the result

$$\tilde{F}(A_{1g})=(\sqrt{2}f_1,\sqrt{8}f_4,\sqrt{8}f_2,\sqrt{8}f_3,2f_6,\sqrt{2}f_5) \ , \tag{21}$$

where $\tilde{F}(A_{1g})$ is the row matrix being the transposition of $F(A_{1g})$. Obviously in the calculation of static displacement using Eq. (16) only the A_{1g} mode is involved with the calculation of the defect-lattice Green's function G confined to the 6×6 matrix $G(A_{1g})$. Consequently, the column vector containing static displacement has exactly the same structure as $F(A_{1g})$ with f replaced by d. Thus the independent components of displacement are $d_z(0,0,x)$, $d_y(0,1,1)$, $d_z(0,1,1)$, $d_x(1,1,0)$, $d_z(0,0,2)$ and $d_y(0,2,0)$.

In the calculation of the defect-lattice Green's function in the A_{1g} mode we need the single element $\Phi_{CC}(A_{1g})$ and the 1×5 matrix $\Phi_{CR}(A_{1g})$ in addition to 5×5 perturbation and Green's-function matrices $V_{RR}(A_{1g})$ and $\mathring{G}(A_{1g})$. Being lengthy, the results are not reproduced here.

In order to calculate the static displacements the required static lattice Green's functions for Cu, Ag, Au, Al, and Ni are those calculated earlier.[40] The Green's functions were calculated with the modified method of Gilat Raubenheimer[41] using phonon data obtained on the basis of force models derived from Born–von Kármán fits to the measured dispersion curves in neutron-scattering experiments. To calculate the forces and perturbation matrix the interaction between a pair of atoms in the defect space is assumed to be given by a Morse potential

$$\Phi(r)=D(e^{-2\alpha(r-r_0)}-e^{-\alpha(r-r_0)}) \tag{22}$$

truncated at the second-neighbor distance in the ideal lattice. The values of D,α,r_0 are chosen according to Cotterill and Doyama[42] to fit the lattice constant, bulk modulus, and vacancy formation energy. For Al and Au we have used the Morse constants obtained by Cotterill and Doyama[42] while for Cu, Ag, and Ni we have obtained these constants following the method outlined by these authors. The Morse constants in Cu have been recalculated primarily because of the changed value of the vacancy formation energy, which is 1.28 eV compared to the 1.17 eV used earlier.[42] The values of Morse constants are given in Table I along with calculated and experimental values of elastic constants. This table also contains first and second derivatives of potentials at first- and second-neighbor distances and the temperature of self-interstitial migration.

Though the use of equilibrium pair potentials is generally accepted to be inadequate for metals and it is far better to use the nonequilibrium potentials,[43] the Morse potential for the fcc metals has been preferred due to the following considerations. In calculating static displacements one of our aims is to compare the present results on the basis of the Green's-function method with the existing computer-simulation studies and lattice-statics calculations. Naturally, therefore, we have chosen the same potential functions as used in previous studies so as to make the comparison meaningful. As a matter of fact, out of many pair potentials available for fcc metals, we have utilized the Morse potential because this potential was used in all the three previous studies with which detailed comparison is possible. However, to get a feeling for the behavior of static properties using different forms of potential we have repeated the calculation for Cu and Au with a nonequilibrium potential constructed by Heugten.[44] The choice of copper and gold has been made for two distinct reasons: while the results for copper are treated as typical of fcc metals where detailed comparison with previous work is possible, the case of gold is anomalous (see below).

The separation of the two atoms forming the dumbbell is determined by minimizing the formation energy of the defect. In all the fcc metals it is $0.57a$, where a is the lattice constant. The calculated displacement and other properties: formation energy, relaxation volume, and dipole tensor, are presented in Table II. It is seen that the nature of displacements is the same in all the metals: strongest outward relaxation of nearest atoms like (0,1,1) followed by inward relaxation of atoms like (1,1,0), the

TABLE I. Morse constants and some properties of fcc metals. The elastic constants are in 10^{12} dyn/cm^2, the first derivatives of potential $\Phi'(r_i)$ are in eV/Å, and the second derivatives $\Phi''(r_1)$ in eV/Å^2. The quantities within parentheses refer to the Heugten potential (Ref. 44). T^M denotes the onset temperature of interstitial migration.

				Calculated		Experimental[a]							
	D (eV)	α (Å^{-1})	r_0 (Å)	C_{11}	C_{12}	C_{11}	C_{12}	C_{44}	$\Phi'(r_1)$	$\Phi'(r_2)$	$\Phi''(r_1)$	$\Phi''(r_2)$	T^M (K)[b]
Cu	0.195 197	2.221 002	2.574 343	1.762 286	1.020 013	1.762	1.249	0.818	−0.056 04	0.079 25	2.294 08	−0.156 16	38
									(−0.117 95)	(−0.014 01)	(1.926 40)	(−0.026 02)	
Ag	0.175 331	2.162 001	2.899 551	1.315 412	0.744 253	1.315	0.973	0.511	−0.039 36	0.055 67	1.890 36	−0.109 91	28
Au	0.158 020	2.840 901	2.882 197	2.014 209	1.077 895	2.016	1.697	0.454	−0.022 52	0.030 18	2.741 08	−0.082 64	<2
									(−0.791 25)	(−0.482 68)	(2.275 70)	(0.222 58)	
Al	0.119 306	2.353 643	2.864 944	0.661 864	0.372 193	1.143	0.619	0.316	−0.019 28	0.033 70	1.456 52	−0.073 897	35
Ni	0.217 829	2.543 00	2.504 475	2.613 419	1.472 810	2.612	1.508	1.317	−0.068 15	0.096 37	3.295 70	−0.207 646	56

[a]Reference 55.
[b]Reference 15.

TABLE II. Displacements (units of $a/2$), formation energies, relaxation volumes, and dipole tensors (in eV) of the ⟨001⟩ dumbbell in fcc metals.

		Dumbbell position	$d_y(0,1,1)$	$d_z(0,1,1)$	$d_x(1,1,0)$	$d_z(0,0,2)$	$d_x(2,0,0)$	E_f (eV)	ΔV (V_c)	P_{11}	P_{33}	TrP	$(P_{33}-P_{11})$/TrP
Cu	(Morse)	(0,0,0.571)	0.1018	0.0453	−0.0424	−0.0319	0.0143	3.617	2.115	18.90	20.91	58.71	0.034
	(Heugten)	(0,0,0.570)	0.0815	0.1232	−0.0589	0.0261	−0.0216	2.422	1.333	12.39	16.66	41.44	0.103
Ag		(0,0,0.572)	0.0923	0.0600	−0.0614	−0.0205	0.0054	5.180	2.448	23.08	25.98	72.15	0.040
Au	(Morse)	(0,0,0.571)	0.0753	0.0601	−0.0906	−0.0220	0.0038	16.884	4.651	65.43	72.29	203.15	0.034
	(Heugten)	(0,0,0.580)	0.1740	−0.1570	0.0122	−0.1441	0.1161	8.171	0.669	10.73	16.40	37.85	0.1498
Al		(0,0,0.571)	0.0813	0.0696	−0.0559	−0.0168	0.0035	5.102	4.683	21.66	23.85	67.16	0.033
Ni		(0,0,0.571)	0.0900	0.0674	−0.0504	−0.0094	0.0014	5.879	2.289	27.88	31.36	87.12	0.040

nearest axial atom (0,0,2) experiences a small inward relaxation whereas (2,0,0) experiences a very small outward relaxation. The formation energy is 3–6 eV except in gold where it is anomalously high ($\simeq 17$ eV). The relaxation volume $2-5V_c$ ($\equiv$atomic volume) is seen to be high compared to experimental values in Cu ($1.45V_c$) (Ref. 45) and Al ($1.9V_c$);[46] it is especially very high in Al and Au. The dipole tensor is nearly isotropic in all the metals with small anisotropies, $(P_{33}-P_{11})/\mathrm{Tr}P$, of 0.03–0.04, a result in agreement with the calculation of Schober[32] and the experimental results, but the sign of the anisotropy is at variance with negative values obtained in Cu and Al from x-ray diffuse scattering between Bragg reflections.[47] Again the dipole tensor is anomalously high in the case of gold. In this context we note that the calculated elastic constants, especially C_{12}, are much different than experimental values in gold and aluminum (see Table I) and to that extent the used potentials for these metals are not very suitable, since for the Morse potential the equilibrium condition is satisfied the Cauchy relation holds, i.e., $C_{12}=C_{44}$, the deviation from the Cauchy relation will indicate the suitability or otherwise of the chosen potential. From Table I it is seen that the deviation $C_{12}-C_{44}$ is maximum for the gold. Clearly an equilibrium potential for gold is not suitable.

Unsuitability of the equilibrium potential aside, the gold is otherwise anomalous. Even with the Heugten potential the results in gold are not very encouraging: while the formation energy and dipole tensor are much in line with other metals the nature of the displacement field is completely changed with a very high magnitude of distortion. All these go to show the anomalous behavior of self-interstitials in gold which is also reflected in very low migration temperature (<2 K) compared to other fcc metals (Table I). The anomalous behavior of self-interstitials in gold and anomalies in other physical properties of gold can basically be traced to its elastic properties.[11] The low values of shear moduli $(C_{11}-C_{12})/2$ and C_{44} results in a very large ratio of bulk modulus to shear modulus which causes an instability in the lattice and which is also responsible for the instability of the self-interstitials, resulting in anomalous properties which raise serious doubts about the stable configuration of self-interstitials in gold.[48,49] If we compare the displacement field in Cu obtained on the basis of the Morse potential and the nonequilibrium Heugten potential we see that the nature of the displacements is much changed though the equilibrium separations between dumbbell atoms are exactly equal. The reason for such a behavior will be made apparent if we notice the fundamental difference between two types of potentials. The characteristic feature of the Morse potential is that the first-neighbor atoms suffer repulsive force and second-neighbor atoms suffer attractive force in all the metals, whereas both the first- and second-neighbor atoms suffer repulsive forces for the Heugten potential as shown in Table I. This distinction between the two potentials stems from the difference in elastic properties: while for the Morse potential $C_{12}-C_{44}=0$, for the Heugten potential, being obtained from phonon dispersion curves, $C_{12}>C_{14}$.

TABLE III. Displacements, formation energy, relaxation volume, and dipole tensor of the ⟨001⟩ dumbbell in Cu.

	Displacements (units of $a/2$)					E_f (eV)	ΔV (V_c)	TrP (eV)
	$d_y(0,1,1)$	$d_z(0,1,1)$	$d_x(1,1,0)$	$d_z(0,0,2)$	$d_x(2,0,0)$			
Present work (Morse)	0.1018	0.0453	−0.0424	−0.0319	0.0143	3.617	2.115	58.71
Schober[a] (Morse)	0.16	0.08	−0.06	−0.02	0.02	3.81	2.4	67.1
Cotterill and Doyama[b] (Morse)	0.139	0.082	−0.045	−0.005	0.009	3.81	1.34	
Miller and Heald[c] (Morse)	0.130	0.152	−0.114	0.064	−0.026	5.5	1.29	39.26
Scholz and Lehmann[d] (Born-Mayer)	0.167	0.089	−0.046	−0.013	0.020	3.50		
Bullough and Tewary[e] (Born-Mayer)	0.0945	0.0282	−0.0154	−0.0239	0.0280		1.57	

[a]Reference 32.
[b]Reference 42.
[c]Reference 30.
[d]Reference 3.
[e]Reference 29.

As the most widely studied, copper has been chosen for detailed comparison with previous work. In Table III we have presented the calculated displacement field and other properties of self-interstitials in Cu together with values reported by other authors. However, a meaningful comparison is possible only with those results which were obtained using the Morse potential, namely that of Cotterill and Doyama,[42] Schober,[32] and Miller and Heald.[30] Confining to the Morse potential we see that the present results for the displacement field essentially agree with the computer-simulation results of Cotterill and Doyama and Schober in that the sign and relative magnitudes of different Cartesian components are more or less the same in all the three sets. However, there is a serious discrepancy in the displacement of the atoms nearest to the dumbbell, e.g., the present value of $d_z(0,1,1)$ is almost half the values reported by the other two authors. The discrepancy cannot be understood only in terms of possible differences in potentials used and it provides a clear pointer to the inadequacy of the harmonic approximation used in the Green's-function treatment. The same conclusion is drawn from a comparison of results of displacements with the Born-Mayer potential reported by Scholz and Lehmann[3] and Bullough and Tewary[29] who have used the computer-simulation and Green's-function method, respectively. The results for formation energy, relaxation volume, and dipole tensor agree reasonably well with those obtained by Cotterill and Doyama and Schober. As regards comparison with the results of Miller and Heald,[30] who have used the Kanzaki method, we find that in addition to differences in magnitudes of displacements the sign of the displacements of the second-neighbor atoms $[d_z(0,0,2), d_x(2,0,0)]$ is opposite to that obtained in the present calculation and that of Cotterill and Doyama and Schober. This could be attributed to the use of entirely different potential constants by Miller and Heald.

B. ⟨110⟩ dumbbell in a bcc lattice

The forces $F_\alpha(1)$ on the atoms in the defect space are calculated with the help of Eq. (20). The independent Cartesian components having nonzero values are $f_1=F_x(x,x,0)$, $f_2=F_x(1,1,1)$, $f_3=F_z(1,1,1)$, $f_4=F_x(1,-1,1)$, $f_6=F_x(2,0,0)$, $f_7=F_y(2,0,0)$, and $f_8=F_z(0,0,2)$. Using symmetry coordinates the force can be projected in different irreducible subspaces of the defect space. The result involves only A_g irreducible representation

$$\tilde{F}(A_g)=(2f_1,\sqrt{8}f_2,2f_3,\sqrt{8}f_4,2f_4 2f_6,2f_7,\sqrt{2}f_8)\ , \tag{23}$$

where $\tilde{F}$ is the transposition of F. Obviously for the calculation of the static displacements we need 8×8 Green's function $G(A_g)$. The structure of the vector containing static displacements in the defect space is identical with $F(A_g)$, with f replaced by d and consequently we have eight independent components of displacements which include the displacement of the dumbbell atom itself: $d_x(x,x,0)$, $d_x(1,1,1)$, $d_z(1,1,1)$, $d_x(1,-1,1)$, $d_z(1,-1,1)$, $d_x(2,0,0)$, $d_y(2,0,0)$, and $d_z(0,0,2)$.

We have calculated static displacements in Fe, Mo, and W. The required static Green's functions for these metals have been calculated with a modified Gilat and Raubenheimer scheme[41] using phonon data from a fifth-neighbor general-force model derived by Minkiewicz, Shirane, and Nathans[50] for Fe, a third-neighbor axially symmetric model by Woods and Chen[51] for Mo, and a third-neighbor general-force model by Chen and Brockhouse[52] for W. These models have been derived from Born–von Kármán fits to the measured phonon-dispersion curves in neutron-scattering experiments. For the calculation of forces and perturbation matrices we have used the interatomic potentials constructed by Johnson and Wilson[33] (JW) from elastic constants and unrelaxed vacancy-formation energy. The JW potentials are simple and easily applicable in defect calculations. They have been used in calculations of intrinsic point defects in bcc metals and give a correct trend for the defect properties in various metals.[9] In particular, these potentials clearly represent the difference in elastic property between two groups of bcc metals, i.e., between so-called normal metals α-Fe, Mo, and W and superconductors V, Nb, and Ta, a property so very important for the static properties of SIA's. To our knowledge, beyond the pair potentials the embedded atom method[53] is being increasingly used for defect calculation. However, the utility of these so-called N-body potentials for the study of SIA's in bcc metals is doubtful. In fact, using the N-body potentials the obtained result for the configuration of single SIA's in Mo and W (Ref. 54) is at variance with a number of computer-simulation studies[7–9] and experiments.[47] In view of all these the JW potentials are considered to be a representative set at present that describes the crystal properties rather well.

The calculated displacement field is presented in Table IV. The separation between dumbbell atoms is found to be $0.7a$, which is in reasonable agreement with the computer-simulation results of Johnson[6] ($\sim 0.75a$) in Fe, Erginsoy, Vineyard, and Englert[5] ($0.725a$) in Fe, Guinan, Stuart, and Borg[7] ($0.75a$) in W, and Taji *et al.*[9] ($0.75a$) in Fe, Mo, and W. The nature of the displacement field of the ⟨110⟩ split interstitials is the same in all the three metals. The effect of strain, reflected in the magnitude of

TABLE IV. Displacement (in units of $a/2$) of neighbors of the ⟨110⟩ dumbbell in bcc metals.

Dumbbell position	$d_x(1,1,1)$	$d_z(1,1,1)$	$d_x(1,-1,1)L$	$d_z(1,-1,1)$	$d_x(2,0,0)$	$d_y(2,0,0)$	$d_z(0,0,2)$
Fe (±0.492,±0.492,0)	0.1385	0.1145	−0.0231	−0.0537	0.1009	0.0358	−0.0830
Mo (±0.493,±0.493,0)	0.1597	0.0960	−0.0381	−0.0283	0.1064	0.0301	−0.0755
W (±0.496,±0.496,0)	0.1491	0.1136	−0.0309	−0.0305	0.0910	0.0266	−0.0715

TABLE V. Formation energies (eV), relaxation volumes (V_c), and dipole tensors (eV) of the ⟨110⟩ dumbbell in bcc metals. P_1, P_2, and P_3 are eigenvalues of the dipole tensor.

	E_f	ΔV	P_{11}	P_{12}	P_{33}	TrP	P_1	P_2	P_3	$(P_1-P_2)/\mathrm{Tr}P$	$(P_1-P_3)/\mathrm{Tr}P$
Fe	7.786	3.246	28.385	21.572	67.138	113.908	49.957	6.813	67.138	0.3788	−0.1508
Mo	12.396	1.280	38.964	26.321	20.508	98.436	65.285	12.643	20.508	0.5348	0.4549
						79[a]	32[b]	9[b]	38[b]	0.2911[a]	−0.0759[a]
W	17.739	1.220	52.287	37.227	9.275	113.849	89.514	15.060	9.275	0.6539	0.7048

[a]Calculated using experimental values from Ref. 10.
[b]Reference 10.

displacement, is strongest ($0.225a/2$) for the nearest atoms (1,1,1), (−1,−1,1) (−1,−1,−1) and (1,1,−1) which experience repulsion. We note that the magnitude of the displacement of the atoms nearest to the dumbbell atom is less than the reported values of $0.29a/2$ in Fe by Erginosoy, Vineyard, and Englert,[5] a result similar to the ⟨100⟩ dumbbell in fcc metals. This again indicates the inadequacy of the harmonic approximation in the Green's-function treatment.

The formation energy, relaxation volume, and dipole tensor are presented in Table V. The calculated formation energies are too high compared to computer-simulation results of Taji, *et al.*[9] who get 5.312 eV in Fe, 8.066 eV in Mo, and 9.564 eV in W using the same potentials. The relaxation volume in Fe seems to be high whereas in Mo the present value ($1.28V_c$) compares well with the experimental value ($1.1V_c$) of Ehrhart[47] and the calculation of Miller[8] ($0.62V_c$). The calculated dipole tensors have the right symmetry. In Mo, where the experimental values are available,[10] the anisotropy of the dipole tensor, as reflected in $(P_1-P_2)/\mathrm{Tr}P$ and $(P_1-P_3)/\mathrm{Tr}P$, is at variance with the experimental results. The values of the dipole tensor seem, in general, to be high.

We note that the lattice Green's functions have been calculated using phonon-based force constants while for calculating force constants in the defect space use of the pair potentials has been made. Normally in any such point-defect calculation the potential should be consistent with the force-constant model used to generate the perfect-lattice Green's functions. Since the potential function corresponding to the force constant model used for the perfect-lattice description is not known, an alternate and more consistent procedure would have been to use the same pair potentials to calculate the Green's functions. Nevertheless, it was felt that the use of the Green's function calculated from the phonon-based force constants will not introduce major errors since, in practice, it has been found that the different force-constant models for a given metal give quite similar values of the Green's functions.[16,29] In any case, in using phonon-based force constants for the Green's functions the idea is to ensure that the perfect crystal is correctly represented within the harmonic approximation and possible uncertainties remain confined to the force constants in the vicinity of the defect determined on the basis of the pair potentials. However, it is possible that the difference between the phonon-based Green's functions and that deduced from the pair potentials applied to the bulk lattice could be responsible for some of the differences between present results and computer-simulation studies; however, we feel that the major differences result from the neglect of the local anharmonicity near the defect which is expected to be important for strongly perturbing defects like self-interstitials.

VI. CONCLUDING REMARKS

We have presented a group-theoretic analysis of second-neighbor defect models for ⟨100⟩-split interstitials in fcc metals and ⟨110⟩-split interstitials in bcc met-

als with a view that they would be useful in future applications to discuss the dynamical properties of these defects in cubic metals. The models have been applied to calculate the static displacement fields due to split interstitials in a number of fcc and bcc metals. Despite reasonable agreement with other calculations using computer simulation for some of the static properties of these defects, especially in fcc metals, the Green's-function method of lattice statics is seen to be limited by its application based on the harmonic approximation. Apart from using improved potentials an inclusion of local anharmonicity on the lines suggested by Tewary[16] may improve the situation. The defect models are applied to calculate the change of elastic constants due to self-interstitials in fcc and bcc metals and would be presented in a separate paper.

ACKNOWLEDGMENTS

The author is grateful to the University Grants Commission, New Delhi for financial assistance and to Professor A. Salam and the International Atomic Energy Commission for giving him the opportunity to visit the International Center for Thoeretical Physics, Trieste, where some of the computations were done.

[1]J. B. Gibson, A. N. Goland, M. Milgram, and G. H. Vineyard, Phys. Rev. **120**, 1229 (1960).
[2]A. Seeger, E. Mann, and R. V. Jan, J. Phys. Chem. Solids **23**, 639 (1962).
[3]A. Scholz and C. Lehmann, Phys. Rev. B **6**, 813 (1972).
[4]J. R. Beeler, Jr., *Radiation Effects Computer Experiments* (North-Holland, Amsterdam, 1983).
[5]C. Erginsoy, G. H. Vineyard, and A. Englert, Phys. Rev. **133**, A595 (1964).
[6]R. A. Johnson, Phys. Rev. **134**, A1329 (1964).
[7]M. W. Guinan, R. N. Stuart, and J. J. Borg, Phys. Rev. B **15**, 699 (1977).
[8]K. M. Miller, J. Phys. F **11**, 1175 (1981).
[9]Y. Taji, T. Iwata, T. Yokota, and M. Fuse, Phys. Rev. B **39**, 6381 (1989).
[10]W. Schilling, J. Nucl. Mater. **69/70**, 465 (1978).
[11]P. Lucasson, F. Maury, and A. Lucasson, Mater. Sci. Forum **15-18**, 231 (1987).
[12]P. H. Dederichs, C. Lehmann, and A. Scholz, Phys. Rev. Lett. **31**, 1130 (1973).
[13]P. H. Dederichs, in *Proceedings of the Conference on Fundamental Aspects of Radiation Damage in Metals, Gatlinburg, 1975,* edited by M. T. Robinson and F. W. Young, Jr. (U.S. Department of Commerce, Siringfeld, VA, 1976), p. 187.
[14]P. H. Dederichs, C. Lehmann, H. R. Schober, A. Scholz, and R. Zeller, J. Nucl. Mater. **69/70**, 176 (1978).
[15]F. W. Young, Jr., J. Nuc. Mater. **69/70**, 310 (1978).
[16]V. K. Tewary, Adv. Phys. **22**, 757 (1973).
[17]A. A. Maradudin, E. W. Montroll, G. H. Weiss, and I. P. Ipatova, *Theory of Lattice Dynamics in the Harmonic Approximation,* 2nd ed., *Solid State Physics,* Suppl. 3 (Academic, New York, 1971).
[18]D. W. Taylor, in *Dynamical Properties of Solids,* edited by G. K. Horton and A. A. Maradudin (North-Holland, Amsterdam, 1974), Vol. 2, Chap. 5.
[19]R. F. Wood, Methods Comput. Phys. **15**, 119 (1976).
[20]R. F. Wood and M. Mostoller, Phys. Rev. Lett. **35**, 45 (1975).
[21]H. R. Schober, V. K. Tewary, and P. H. Dederichs, Z. Phys. **21**, 255 (1975).
[22]R. Zeller and P. H. Dederichs, Z. Phys. B **25**, 139 (1976).
[23]P. N. Ram and P. H. Dederichs, Z. Phys. B **42**, 57 (1981).
[24]P. N. Ram and P. H. Dederichs, KFA Jülich Report JUL 1725 (1981) (unpublished).
[25]P. N. Ram, Phys. Rev. B **30**, 6146 (1984).
[26]P. N. Ram, Phys. Rev. B **37**, 6783 (1988).
[27]R. Urban, P. Ehrhart, W. Schilling, H. R. Schober, and H. Lauter, Mater. Sci. Forum **15-18**, 243 (1987); Phys. Status Solidi B **144**, 287 (1987).
[28]W. Luding, Ergeb. Exakten Naturwiss. **35**, 1 (1964).
[29]R. Bullough and V. K. Terwary, in *Interatomic Potentials and Simulations of Lattice Defects,* edited by P. C. Gehlen, J. R. Beeler, Jr., and R. I. Jaffee (Plenum, New York, 1972), p. 155.
[30]K. M. Miller and P. T. Heald, Phys. Status Solidi B **78**, 341 (1976).
[31]H. Kanzaki, J. Phys. Chem. Solids **2**, 24 (1957).
[32]H. R. Schober, J. Phys. F **7**, 1127 (1977).
[33]R. A. Johnson and W. D. Wilson, in *Interatomic Potentials and Simulation of Lattice Defects,* edited by P. C. Gehlen, J. R. Beeler, Jr., and R. I. Jaffee (Plenum, New York, 1972), p. 301.
[34]J. A. Krumhansl and J. A. D. Matthews, Phys. Rev. **166**, 856 (1968).
[35]P. H. Dederichs and R. Zeller, Phys. Rev. B **14**, 2314 (1976).
[36]P. H. Dederichs and R. Zeller, in *Point Defects in Metals II,* Vol. 87 of *Springer Tracts in Modern Physics,* edited by G. Hohler and E. A. Niekisch (Springer, Berlin, 1979), p. 1.
[37]The tables of symmetry coordinates are available with the author.
[38]A. A. Maradudin, in *Lattice Dynamics,* edited by S. F. Edwards (Benjamin, New York, 1969), p. 1.
[39]J. R. Hardy, J. Phys. Chem. Solids **29**, 2009 (1968).
[40]P. N. Ram and P. D. Semalty, Phys. Status Solidi B **142**, 387 (1987), and unpublished.
[41]G. Gilat and L. J. Raubenheimer, Phys. Rev. **144**, 390 (1966).
[42]R. M. J. Cotterill and M. Doyama, in *Lattice Defects and Their Interactions,* edited by R. R. Hasiguti (Gordon and Breach, New York, 1967), p. 1.
[43]A. E. Carlson, in *Solid State Physics,* edited by H. Ehrenreich and D. Turnbull (Academic, New York, 1990), Vol. 43.
[44]W. F. W. M. van Heugten, Phys. Status Solidi B **86**, 277 (1978); Ph.D. thesis, Groningen, 1979.
[45]H. G. Haubold and D. Martinsen, J. Nucl. Mater. **69/70**, 644 (1978).
[46]H. G. Haubold, in *Proceedings of the Conference on Fundamental Aspects of Radiation Damage in Metals, Gatlinburg, 1975,* edited by M. T. Robinson and F. W. Young, Jr. (U.S. Department of Commerce, Springfield, VA, 1976), p. 268.
[47]P. Ehrhart, J. Nucl. Mater. **69/70**, 200 (1978).
[48]J. Koehler, in *Point Defects and Defect Interactions in Metals* (The University of Tokyo Press, Tokyo, 1982), p. 143.
[49]J. Koehler, Phys. Rev. B **18**, 5333 (1976).
[50]V. J. Minkiewicz, G. Shirane, and R. Nathans, Phys. Rev.

162, 528 (1967).
[51]A. D. B. Woods and S. H. Chen, Solid State Commun. **2**, 233 (1964).
[52]S. H. Chen and B. N. Brockhouse, Solid State Commun. **2**, 73 (1964).
[53]M. S. Daw and M. I. Baskes, Phys. Rev. B **29**, 6443 (1984); M. W. Finnis and J. E. Sinclair, Philos. Mag. A **50**, 45 (1984).
[54]G. J, Ackland and R. Thetford, Philos. Mag. A **56**, 15 (1987); J. M. Harder and D. J. Bacon, *ibid.* **58**, 165 (1988).
[55]C. Kittel, in *Phonons in Perfect Lattices and in Lattices with Point Imperfections,* edited by R. W. H. Stevenson (Oliver and Boyd, London, 1966).